Degradation investigation and active packaging performance of cross-linked chitosan film containing gallic acid

Submitted to

RSC Sustainability

March 2025

Jessica R. Westlake [†], Edward Chaloner [◊], Maisem Laabei [*], Fotis Sgouridis [⊥], Andrew D. Burrows [‡], Ming Xie [†]

[†]Department of Chemical Engineering, University of Bath, Bath, BA2 7AY, UK.

[‡]Department of Chemistry, University of Bath, Bath, BA2 7AY, UK.

[◊]Department of Biology, University of Bath, Bath, BA2 7AY, UK.

[*]School of Cellular and Molecular Medicine, University of Bristol, Bristol, BS8 1TH, UK.

[⊥]School of Geographical Sciences, University of Bristol, BS8 1QU.

Corresponding authors:

Ming Xie, mx406@bath.ac.uk

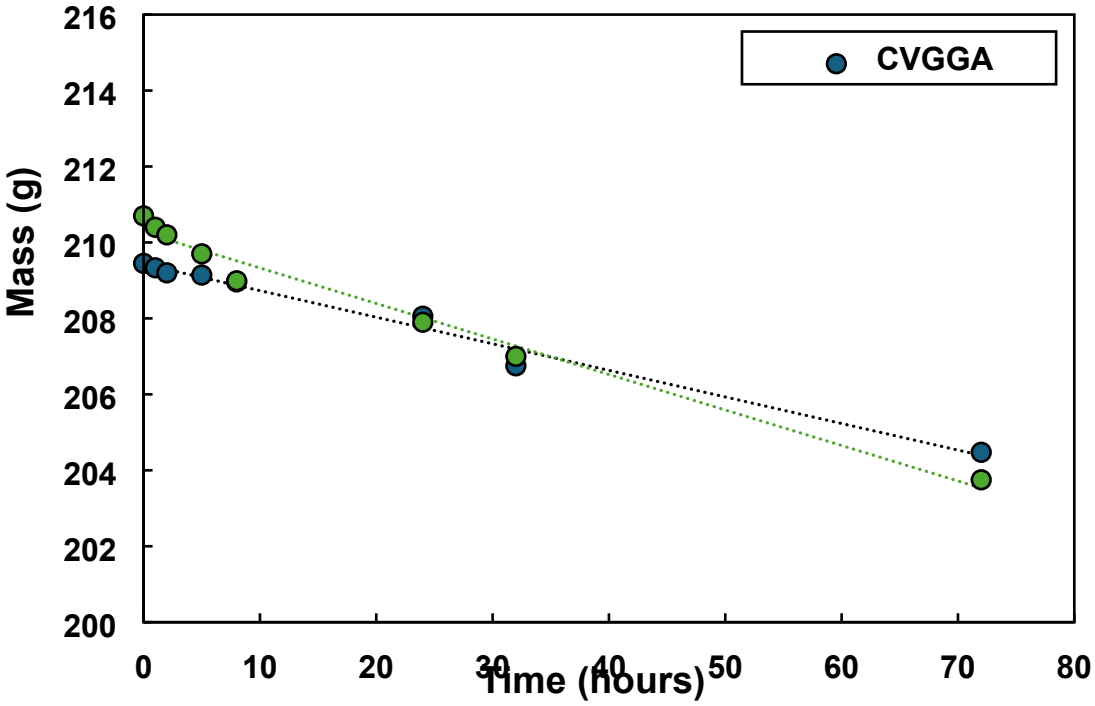

Figure S1. Slopes of the weight loss versus time data for water vapour permeability measurements of CVG and CVGGA films.

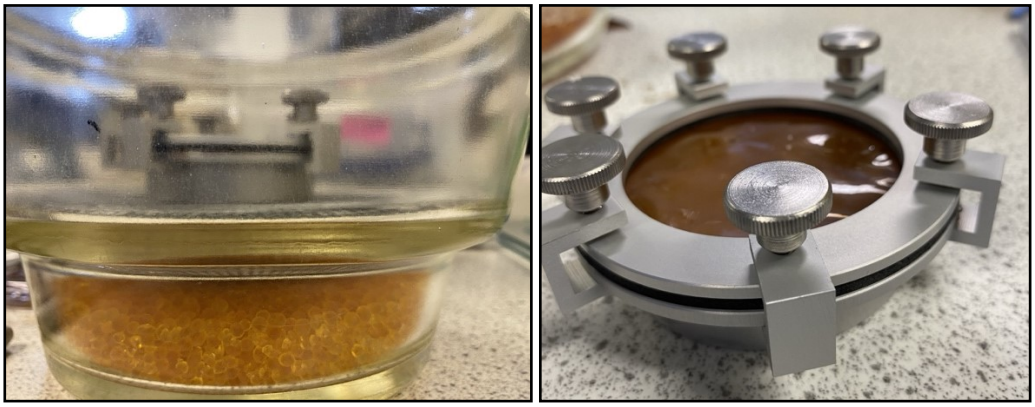

Figure S2. Image of the set-up in the laboratory for water vapour permeability (WVP) experiments using a permeability cup and a glass desiccator with silica beads, maintained at 25.7 ± 1.1 °C and 37.7 ± 3.8% relative humidity, monitored using a digital hygrometer and thermometer.

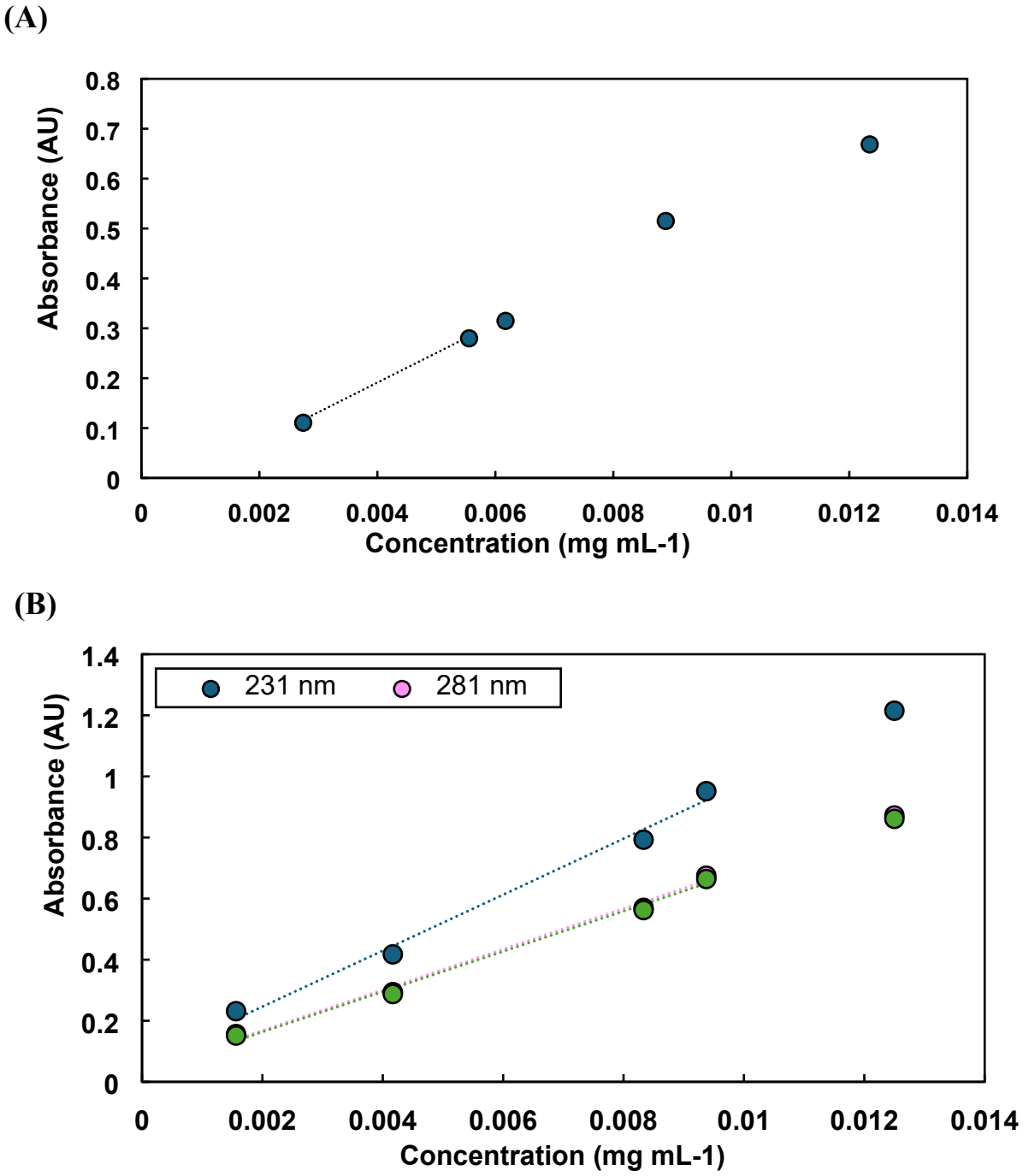

Figure S3. Calibration curves, using stock solutions of (A) gallic acid and (B) vanillin in 95% (v/v) ethanol in water, measured using UV-Visible spectroscopy with a quartz cuvette. Migration experiments of CVG and CVGGA at 275 nm were used to determine the percentage release of gallic acid in comparison to vanillin. These values were utilised to convert the release study data to the release of gallic acid only.

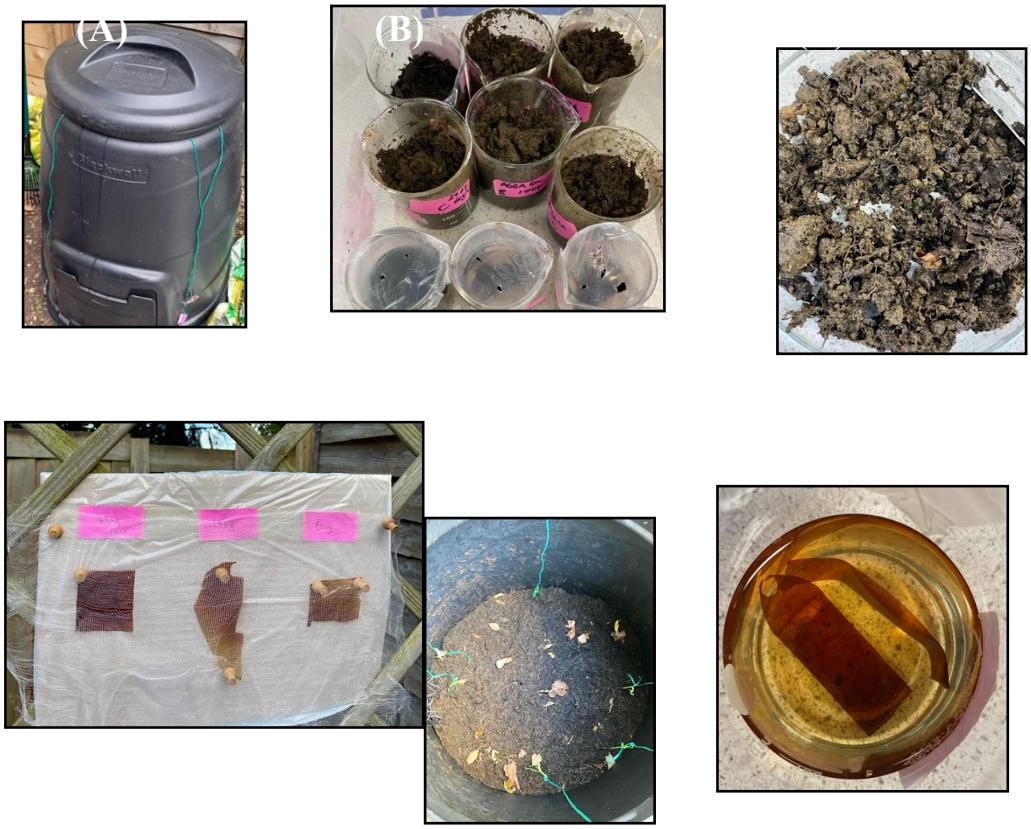

Figure S4. Images of the degradation set-ups (A) the compost bin utilised outside, (B) the set-up for laboratory soil degradation experiments, (C) the soil deposited on a large glass plate to search for degradation products, (D) outside UV degradation set-up, (E) the inside of the compost bin, with samples attached to twine and (F) the seawater degradation experiment in the laboratory.

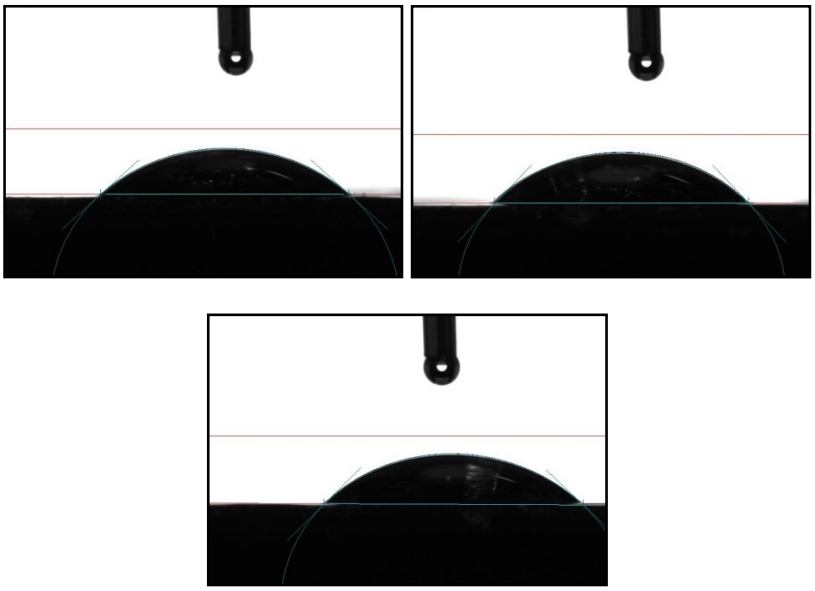

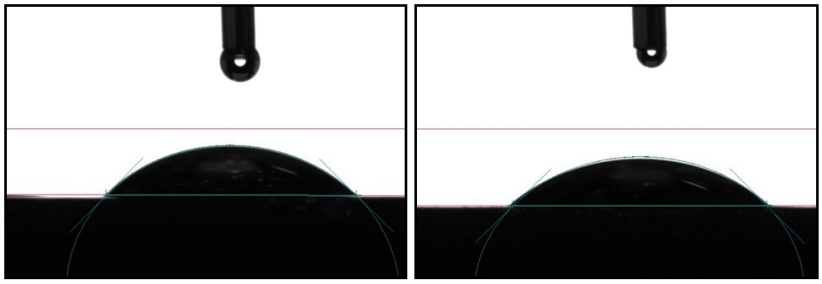

Figure S5. Water contact angle images for CVGGA films, used to calculate an average value.

Figure S6. Image of tensile strength experiments, with masking tape used on the ends of the sample to prevent cracking and slippage.

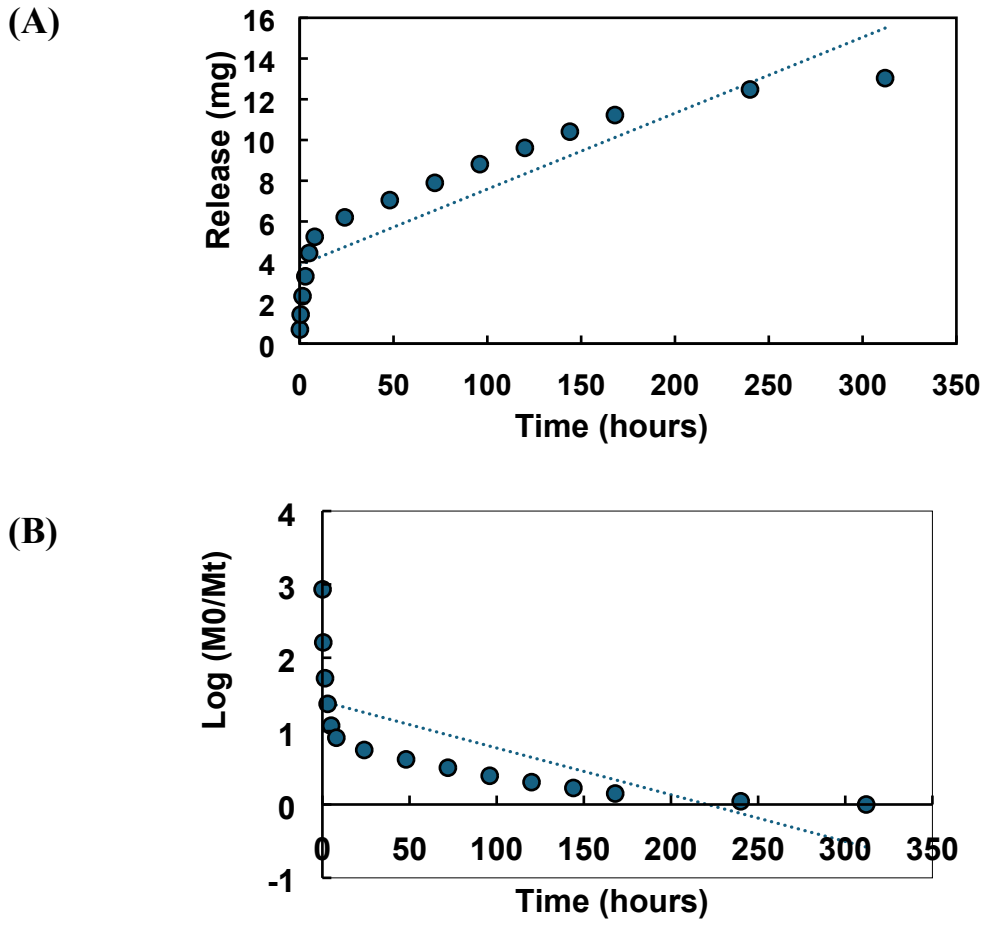

Figure S7. The release profile of gallic acid fit to zero- (A) and first- (B) order kinetics.

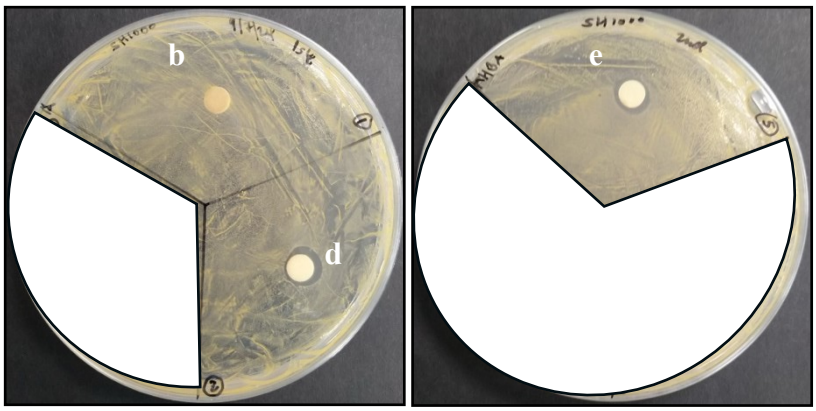

S. aureus

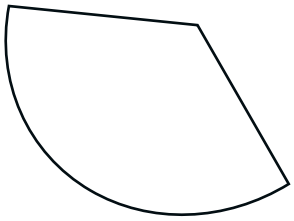

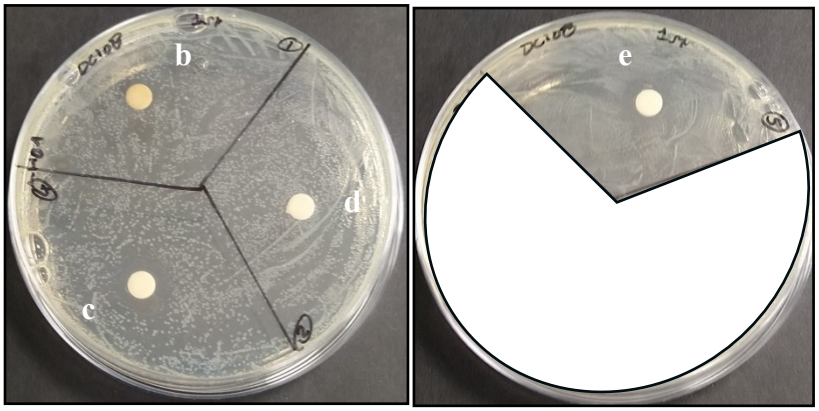

E. coli

Figure S8. Zone of inhibition data for CVGGA film-forming solution (b), CVG film-forming solution (d) and CG film-forming solution (e).

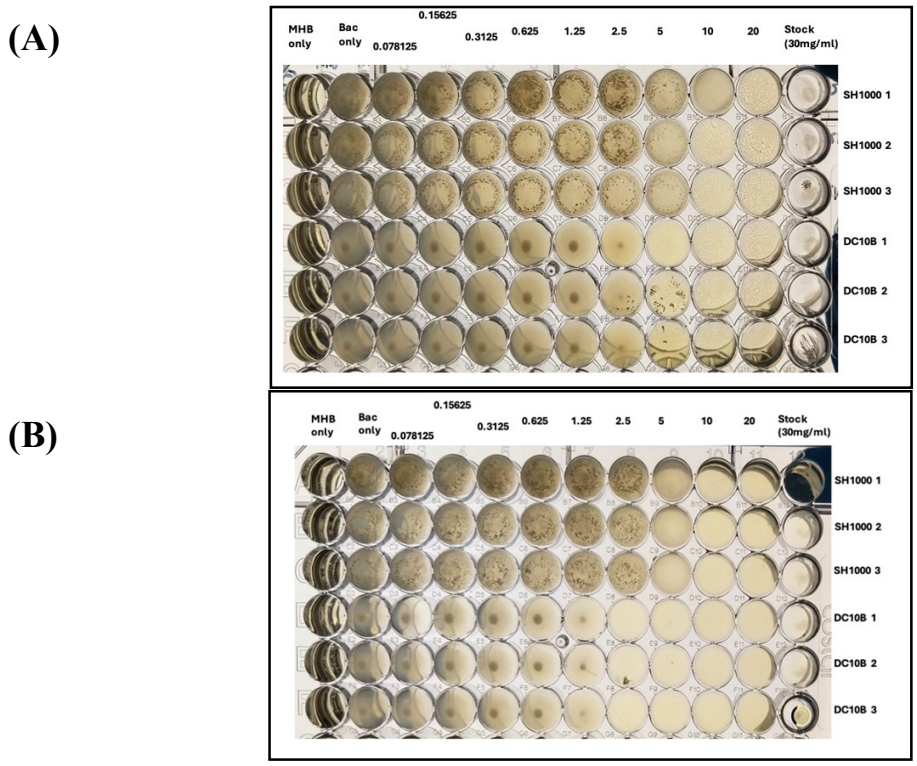

Figure S9. MIC plates of (A) gallic acid and (B) vanillin.

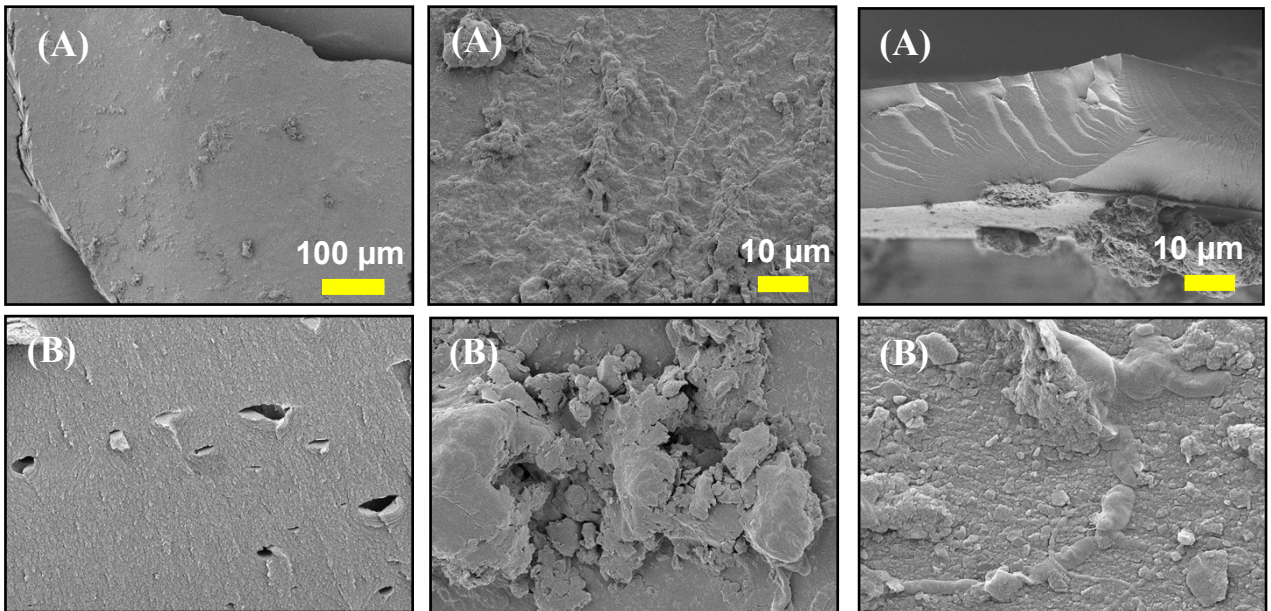

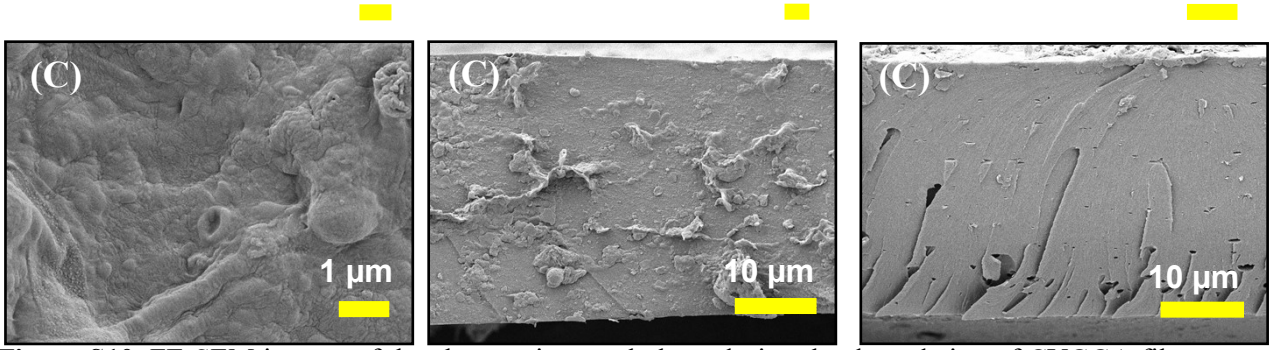

Figure S10. FE-SEM images of the changes in morphology during the degradation of CVGGA films in soil (surface and cross-section) at (A) 3 weeks, (B) 6 weeks and (C) 9 weeks.

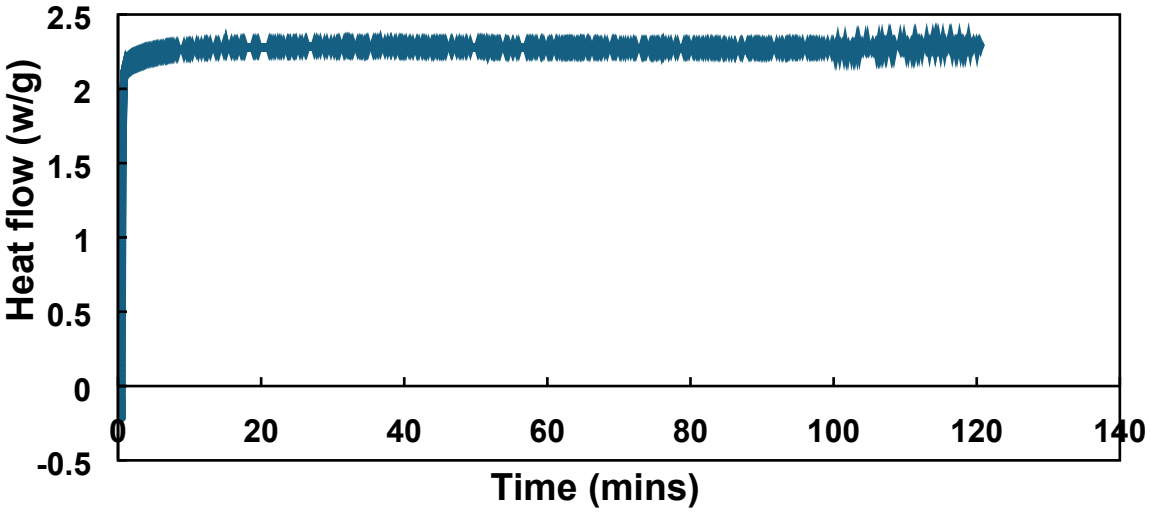

Figure S11. DSC-UV results for CVGGA film held isothermally at 25 °C.

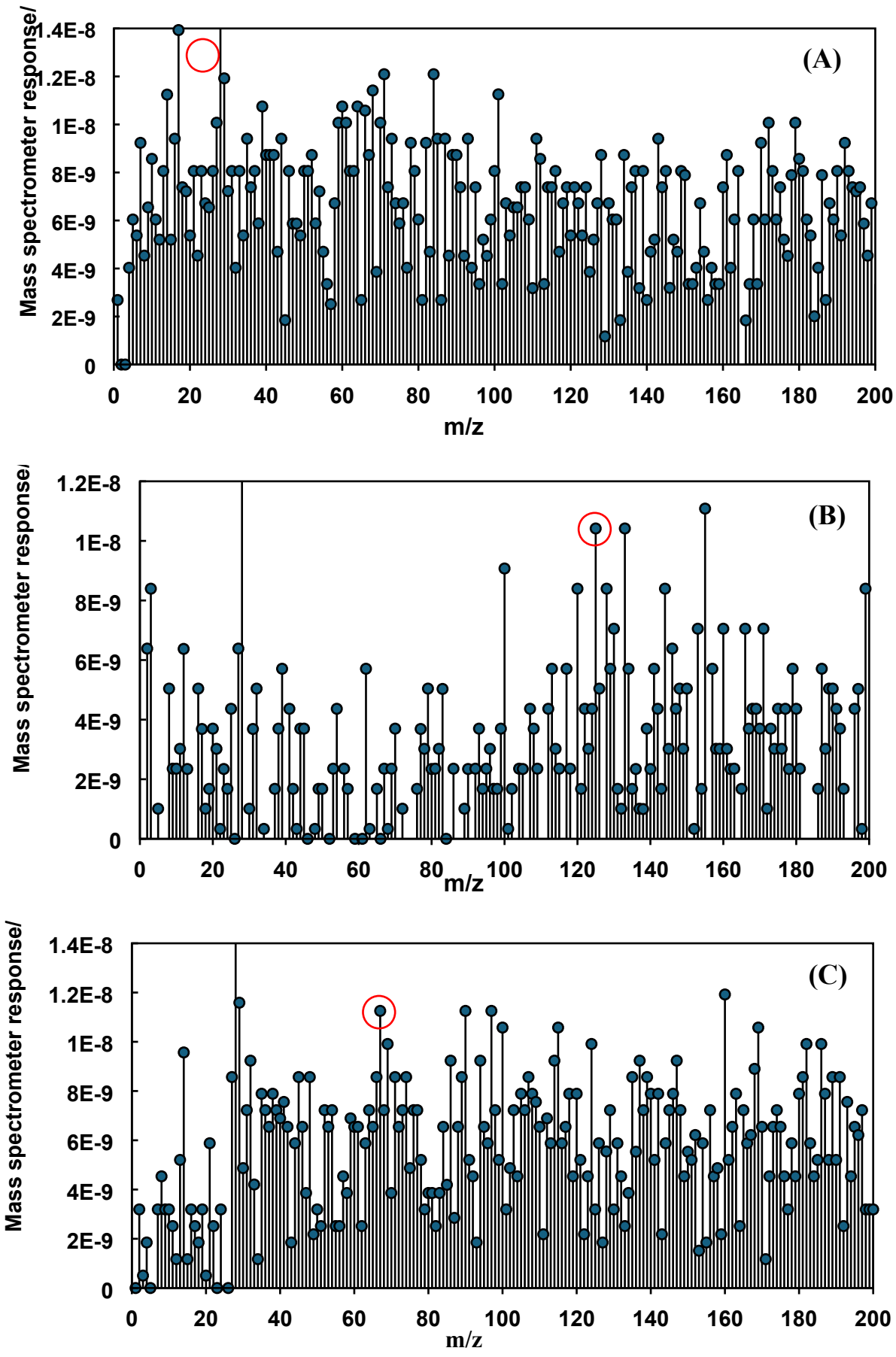
(A)
(B)
(C)
Mass spectrometer response/
m/z
1.4E-8
1.2E-8
1E-8
8E-9
6E-9
4E-9
2E-9
0
0
20
40
60
80
100
120
140
160
180
200

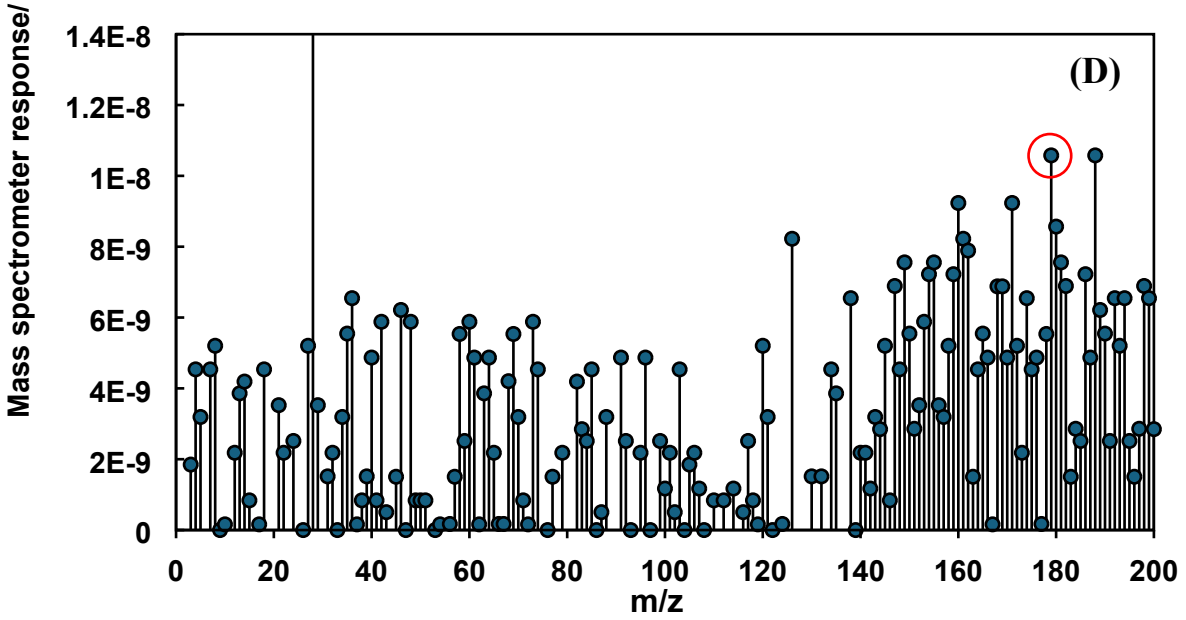

Figure S12. TGA-MS (EGA) data of the pyrolysis of a CVGGA film at (A) 211 °C, (B) 326.5 °C, (B) 406.5 °C and (D) 602.3 °C, with assigned prominent m/z peaks highlighted, the mass spectrometer responses have been normalized against an empty furnace.